Zhai, Z. and Chen, Q. 2005. "Performance of coupled building energy and CFD simulations," **Energy and Buildings**, 37(4), 333-334.

Performance of Coupled Building Energy and CFD Simulations

Zhiqiang (John) Zhai
Department of Civil, Environmental, and Architectural Engineering
University of Colorado at Boulder
UCB 428, ECOT 441
Boulder, CO 80309-0428, USA

Qingyan (Yan) Chen
School of Mechanical Engineering
Purdue University
585 Purdue Mall, West Lafayette, IN 47907-2088, USA

Abstract

The integration of building energy simulation (ES) and computational fluid dynamics (CFD) programs can provide more accurate prediction of building energy use and indoor environment due to the complementary information provided by the two programs. This paper outlines briefly a coupled energy simulation and computational-fluid-dynamics program with different coupling methods and validates the coupled program by using four sets of experimental data from literature. The comparison of the simulated results with the experimental/empirical data reveals the advantages of the integrated building simulation over the separated energy simulation and computational-fluid-dynamics applications. Then the program was used to calculate the cooling load of a large-scale indoor auto-racing complex.

1. Introduction

Energy simulation (ES) and computational fluid dynamics (CFD) programs are two important building design tools. The information provided by them is essential for the evaluation of the most significant building performance, including thermal comfort, indoor air quality, mechanical system efficiency, and energy consumption. Based on the information, a building designer is able to modify his/her design toward an optimal solution. The information provided by ES and CFD programs is complementary, as partially demonstrated by Table 1. The integration of these two tools can eliminate the primary assumptions employed in the separate simulations and thus results in more accurate predictions of building performance. For instance, an ES program can provide building heating/cooling load and interior surface temperatures of building envelopes to CFD as boundary conditions while CFD can determine surface convective heat fluxes for ES.

Zhai and Chen (2002a and 2002b) discussed principles, strategies and methods for coupling ES and CFD. This investigation implemented these concepts and developed an integrated building design tool, E+MIT-CFD, by incorporating a CFD program (MIT-CFD) into an ES program (EnergyPlus) (Crawley 2000). The investigation has focused on the thermal coupling of the ES and CFD programs, without considering their connections at mechanical system and plant levels. In such thermal coupling, ES provides heating/cooling energy required and building envelope thermal information, such as surface temperature and heat flux, to CFD as

boundary conditions; CFD predicts detailed room air temperature distributions and accurate convective heat transfers that help ES to calculate more accurately total energy consumption in a building. This paper first outlines a coupled ES and CFD program that has various coupling methods. It then reports the validations of the program by the experimental data from four full-scale buildings and the application of this program for the cooling load calculation of a large-scale indoor auto-racing complex.

2. Implemented Coupling Strategies and Methods

In a coupled CFD-ES simulation, CFD accounts for the major computing time due to the iterative calculation of the flow governing equations. The long computing time restricts the applicability of the coupling program for practical design purpose. Zhai and Chen (2002a) proposed several staged coupling strategies to reduce the computing time. Figure 1 expands the coupling strategies to be *static coupling process*, *dynamic coupling process*, and *bin coupling process*.

The static coupling process has one-step or two-step data exchange between ES and CFD programs. With only a few coupling iterations, the static coupling can be performed manually, which does not require arduous modifications of individual ES and CFD programs.

The dynamic coupling process involves continuous coupling between the two programs at each time step, which can be further divided into three different categories. The first one is one-time-step dynamic coupling process that focuses on the coupling at one specific time step of interest. At that time step, the iteration between ES and CFD is carried out to reach a converged solution. The second one is quasi-dynamic coupling process, in which ES and CFD couple each other without iteration at each time step in a period of time. That is, CFD receives the boundary conditions from the previous ES calculation at the n^{th} time step and returns the thermal information of indoor air to ES of the next $(n+1)^{th}$ time step. The third one is full dynamic coupling process that iterates ES and CFD a number of times at each coupling time step to reach a converged solution before moving on to the next time step.

The bin coupling process is designed to further reduce the computing cost. It provides ES the information that is pre-computed by CFD and saved in the bins for continuous energy calculation. Two bin coupling processes – static bin coupling process and dynamic bin coupling process – have been developed. In a static bin coupling, the indoor air thermal information required by ES are pre-calculated by CFD as the functions of cooling/heating loads (for conditioned periods) or indoor-outdoor air temperature difference (for unconditioned periods). ES then determines the parameters for a particular simulation by directly interpolating the CFD results from the static function bins. Dynamic bin coupling, rather than generating curve-fitted functions and establishing a comprehensive bin system in advance, predicts the airflow details in some typical days by either quasi-dynamic or full dynamic coupling process. These results are then used in ES for the days with similar conditions.

The present coupling program has implemented all the proposed coupling strategies in E+MIT-CFD. In practice, the building characteristics and the purpose of simulation determine

the most suitable coupling process for a particular building. Sometimes, several coupling processes may be used together to achieve the best solution for a specific case.

In all of the above coupling processes, the convective heat from building enclosures has been demonstrated to be the key link between ES and CFD (Zhai and Chen 2002b). The theoretical analysis and numerical experimentation verified that different data coupling methods of the convective heat transfer have different impacts on the accuracy, convergence, stability, and computing time of a coupled simulation. Table 2 summarizes the available data coupling methods between ES and CFD and qualitative comparison of their performance. As concluded by Zhai and Chen (2002b), coupling method-1, which transfers enclosure interior surface temperatures from ES to CFD and returns convective heat transfer coefficient and indoor air temperature gradients from CFD to ES, is more reliable and efficient than other coupling methods. The method can unconditionally satisfy the convergence condition. It also results in an explicit iteration in ES which is faster and more stable in computation than the implicit iteration. Hence, this study has mainly used coupling method-1, although the other data coupling methods have also been implemented into the coupling program, E+MIT-CFD, for comparison.

3. Validations of the Coupling Program

The new coupling program has been validated with available experimental data to demonstrate the benefits of coupled simulations over separate applications and test the performance of different coupling strategies. The validation cases are:

(1) Natural convection in a room without radiator (Lomas et al 1994);
(2) Natural convection in a room with a radiator (Lomas et al 1994);
(3) Convective heat transfer coefficients in a room with a radiator (Wallenten 1998);
(4) Mixed convection in a glazed atrium (Hiramatsu et al 1996).

(1) Natural convection in a room without radiator

The study first validates the coupling program by using the International Energy Agency (IEA) Annex 21/Task 12 test facility (Lomas et al. 1994). The facility was built for providing reliable experimental data for empirical validation of building energy simulation programs. Considerable differences among the results of different energy simulation programs have been found and few predictions can lay within the error bands for all the measured data. This study simulates the case with double glazing south window to test the dynamic coupling of E+MIT-CFD program.

Figure 2 shows the model of the test facility built with the geometry and materials information from the IEA report. The model consists of two zones – test room and roof space. The envelopes of the facility are exposed to the outdoor environment except the west wall that is adiabatic because of the identical adjacent room. Exterior shading from the neighboring test buildings is also included by using a detached shading surface. Detailed modeling algorithms for solar radiation, building envelopes and indoor air in EnergyPlus (Crawley et al. 2000) were employed in the energy simulation with a ten-minute time step, under the actual outdoor climate conditions for the experimental period (May 21-30, 1990). In a coupled simulation, CFD only

modeled the test room, which was divided into 14×21×19=5,586 non-uniform grid cells. The coupled simulation used the full dynamic coupling strategy with data coupling method-1 to exchange information between ES and CFD. The coupling frequency was set at each hour for all the ten days. The first three days worked as the warm-up period of the simulation and the results of the rest seven days were analyzed. The total computing time of the coupled simulation is about 1 hour 45 minutes on a PIII-900MHz desktop PC when using a zero-equation turbulence model (Xu and Chen 1998) in CFD.

Figure 3 shows the variation of indoor air velocity and temperature in the middle plane of the room at four different moments in a typical test day, computed by CFD with the real-time boundary conditions obtained from ES. The figures exhibit how the outdoor conditions influence the indoor airflow patterns through the window. The indoor air temperature, although not completely uniform, has a very small gradient within the room throughout the day. The same uniform temperature patterns were observed in the measurement, which implies that the uniform air assumption of ES may be acceptable for this case.

The study compares the measured and computed air temperature at the center of the room, as shown in Figure 4(a). The result reveals that EnergyPlus can produce reasonable solutions for this case even without coupling. The coupled results agree better with the data by capturing a more accurate peak room temperature in the later afternoon. As a comparison, Figure 4(b) presents the computed results by Negrao (1995) who used a different coupled ES and CFD program. Their conclusions are similar to ours although the CFD models are different.

To reduce the computing time of the coupled simulation, the dynamic bin coupling strategy was used for this case. In the dynamic bin coupling, the hourly quasi-dynamic coupling process was employed to model the first three days where the first two days were warm-up periods of the simulation. The dynamic results of indoor air temperature gradients and convective heat transfer coefficients in the third day were saved and used in the energy simulation for the next seven days. This dynamic bin coupling strategy with quasi-dynamic coupling process significantly reduces the computing time to about 15 minutes for the whole simulation with the same computer. The results are very close to those produced with the full dynamic coupling for all ten days, as shown in Figure 4(a). This is because the dynamic characteristics of airflow and heat transfer in the ten days are very similar due to the similar environmental and operational conditions.

(2) Natural convection in a room with a radiator

The simulation of the natural convection room without internal heating objects provides reasonable results even without the coupling because of the acceptable convection coefficient correlations used and uniform indoor air temperature. A room with a radiator, however, would impose much more challenges. The literatures (e.g. Lomas et al. 1994) report some interesting observations about the simulated and measured results:

- Most ES programs under-predicted the energy consumption.
- Predicted energy consumption varied considerably between programs (52% variance in the case of the double-glazed room).

- Most programs under-predicted the lowest and highest temperatures in the test room.

The IEA report (Lomas et al. 1994) analyzed that the modeling of internal convection and the influence of temperature stratification are probably two of the primary causes for the discrepancies between the different ES programs and between simulated and measured results. This study models the test room with an oil-filled electrical panel radiator placed under the south window. The average maximum power output of the radiator was 680W. The heat output from the radiator was 60% radiative and 40% convective. In the experiment, the dynamic response of the radiator was represented by a first order system with a time constant of 22 minutes.

This investigation has modeled the radiator using the "High temperature radiant system" model of EnergyPlus. Since the actual PID controller used in the experiment cannot be modeled by EnergyPlus, an operative temperature throttling range of 26-30°C, corresponding from full to zero power, was used to control the radiator. The simulation has been performed under the real weather conditions of the test days (October 17-26, 1987). The hourly full dynamic coupling simulation has been performed for the ten consecutive days. The total computing time of the coupled simulation is about 3 hours 50 minutes with a PIII-900M desktop PC.

The calculated and measured mean air temperatures over a single day (October 23) are compared in Figure 5. In the experiment, the heater turned on at 6:00 but it would not heat up the air around the sensors in the room to the set-point temperature of 30°C until approximately 11:00. This is because the radiative portion of the heat output would be absorbed by the internal surfaces before convecting into the air, resulting in a time lag in the response of the air temperature to heat injection. Both coupled and non-coupled simulations have captured the same heat transfer mechanics, although smaller lag times were computed. The computed air temperature from the coupled simulation is closer to the measured data than that from the non-coupled simulation. The result from the current investigation is slightly better than that obtained by Beasoleil-Morrison (2000) who used the ESP-r program with CFD whose results are also presented in Figure 5.

The small lag time (the computed result is about 1 hour leading the measured value) is probably caused by the current ES program that cannot properly model the dynamic behaviors of the oil-filled radiator. With the present "step-function" radiator model in EnergyPlus, the time delay of power/temperature when the heater is switched on or off cannot be represented. It results in the fast temperature rise and drop in the simulation. This can be partially verified by testing the case with different convective/radiant splits. Our study has found that the case with 0% radiant and 100% convective split almost has no time lag to affect the indoor air temperature while even the case with 100% radiant and 0% convective split still has a shorter time lag than measured one. Moreover, when the heater turns off at 18:00, the indoor air temperatures of all the three simulations drop immediately without delay.

Figure 6 presents the daily-averaged convective heat transfer coefficients at floor, ceiling, south window, and north wall from the coupled and non-coupled simulations as well as those estimated using Khalifa correlations (1989). The coupled results are closer to Khalifa correlations that were particularly developed for the radiator-heating scenarios. Beausoleil-

Morrison (2000) indicated that Khalifa correlations overestimate the h value for the window above the radiator.

Although distinct convection coefficients and air temperature stratification were obtained by the coupled simulation, our simulation still under-estimated the energy consumption by radiator that was 70.4 MJ for seven days, 21.2% less than the measured value of 89.4 MJ. The uncertainty bands of the measurement were reported to be from 78.1 MJ to 92.7 MJ. The coupled result has slight improved by comparing it to the non-coupled simulation that was 66.5 MJ. Olsen (2002) obtained very similar results by using EnergyPlus. He explained that this is primarily attributed to the lack of any time lag in the radiator model, which allows the air to heat up faster than it actually does, and thus allows the radiator energy consumption to decrease more rapidly.

(3) Natural convection coefficients in a room with a radiator

Furthermore, our experience on the IEA validation cases reveal that the convective heat transfer coefficients computed by CFD are much larger than those from the correlations in ES. Although the credibility of the convective heat transfer coefficients computed by CFD with simple zero-equation turbulence models have been examined (Zhai and Chen 2003), it is always desired to have the knowledge of the dynamic behaviors of the coefficients under real building operating conditions.

Few experimental data exists for the validation of the convective heat transfer coefficient calculation under dynamic operational conditions, rather than well-controlled laboratory conditions. Wallenten (1998) conducted such an experiment in a full-size test room located in Lund, Sweden, which has the roof and the south wall with a 1×1.1m window exposed to the ambient. The experiment monitored the surface, air and interstitial wall temperatures. Convection coefficients were then derived from these data using a surface heat balance that considered convection, internal long wave radiation, and conduction through the wall. However, because the dynamic heat conduction and internal long wave radiation were taken into the consideration as they were to represent the realistic operating conditions, the uncertainty to the calculation of convective heat transfer coefficients, h, is significant. For example, the accuracy of h is at best ±15% for the window and ±20% for the walls. As a result, the scattered data are not suitable for quantitative comparison but they do demonstrate the matched trend or range between the simulated and measured results.

This study investigated the Wallenten's unventilated case with a normal 3-pane south window. A small radiator was placed either 0.2 m from the north (back) wall in the center of the wall or 0.12 m from south wall under the window. In the experiment, the radiator was controlled by its own bimetallic thermostat that allowed the average effect at 180W. In the simulation, the radiator was modeled using the "High temperature radiant system" model with 60/40 convective/ radiative split. Since the radiator was turn on for the whole days, the time lag deficiency of the model becomes less important.

The study applied both non-coupled and coupled simulation to three different scenarios: (1) radiator-off; (2) radiator-on under the window; and (3) radiator-on at the back wall. The

simulations were conducted for a seven-day experimental period in January with a ten-minute time step in ES. A climate file typical of the region was employed as no Lund weather data was available for the period of the experiments. The CFD simulation in the coupled program divided the indoor space into 26×29×24=18,096 non-uniform grid cells. The zero-equation turbulence model (Chen and Xu 1998) was used to simulate the turbulence. The hourly full dynamic coupling with data coupling method-1 was adopted for all the seven days. The total computing time of the coupled simulation is about 7 hour and 30 minutes with a PIII-900M PC.

The experimental results show that the location of the radiator has a significant impact on convective heat transfer coefficients at the window. Much higher h_c values were observed when the radiator was placed under the window than when it was placed at the back wall. Quantifying the differences is difficult due to the data scatter, but Wallenten recommends a multiplier as high as 3.5. The simulated results are presented in Figure 7, where the convective heat transfer coefficient, $h_c = q_c / (T_{ref} - T_{surface})$ and T_{ref} is the air temperature at the center of the room. Apparently, the usage of the same correlations in ES cannot distinguish the h_c values between the case with the radiator under the window and the case with the radiator at the back wall. The h_c values provided by CFD are much higher than those from the correlations, with greater values occurring when the radiator is placed under the window. The difference is about 2 times, which is less than the observation but much more obvious than the simulated results by Beausoleil-Morrison (2000) who used the adaptive h_c correlations of the ESP-r program during the simulation.

Figure 8 illustrates the computed and measured h_c at the south wall when the radiator is placed at the back wall. The experiment observed that the heat output from the radiator significantly affected the convective regime and much higher h_c values were found when the radiator was operating. The simulation without coupling cannot capture this phenomenon because of using the same correlations for all the scenarios. The coupled results reveal the distinct separation of h_c values between the radiator-on case and radiator-off case. The results show good agreement with the experimental data and with the simulated results from Beausoleil-Morrison (2000) who used the artificial toggle of the h_c correlations according to the radiator's operational state.

(4) Mixed convection in a glazed atrium

The study further validated the coupled program for a ventilated room. The experimental facility used is a full-scale glazed atrium in Japan (Hiramatsu et al 1996). Figure 9 illustrates the geometry and the configuration of the atrium. The atrium has a glazed ceiling, south, west, and east walls while the floor and the north wall were insulated. The present investigation studies only a cooling scenario using opening A to supply cool fresh air and using opening B to exhaust warm indoor air. All the other openings were closed. The cooling system for the atrium had a maximum power of 32 kW and the maximum air supply volume of 4050 m^3/hr. The atrium was empty and had no partitions. The experiment with the air cooling conditions was conducted on April 5th, 1994. Plenty of measurement data has been collected and widely used to validate simulation programs.

This study simulated the experimental day and the previous warm-up days with ten-minute time steps in ES. Detailed coefficient correlations of EnergyPlus were used in the ES only simulation. In the coupled simulation, CFD has modeled the space with two sets of non-uniform grids: 19×10×14 = 2,660 and 31×18×27 = 15,066 cells. The hourly full dynamic coupling with coupling method-1 was operated for the experimental day only (not for the warm-up days) to reduce the computing cost. The results with the two grids are similar, indicating the grid-independence of the solutions. The total computing time of the coupled simulation with the coarse grid distribution is about 1 hour 30 minutes with the PIII-900MHz PC.

The results show that the ES only simulation underestimates the convective heat from the enclosures. As an example, Figure 10(a) demonstrates the convective heat from the south window with different simulation approaches. A significant difference of the convective heat is noticed, especially around noon time when the difference is about 2 times. As a consequence, the window interior surface temperature from the coupled simulation is lower (closer to the measured value) than that from the non-coupled simulation, as shown in Figure 10(b). The distinction of the window temperature between the two approaches is not as much as that of convective heat, indicating the radiation between surfaces contributes significantly in this case.

With the real-time boundary conditions provided by ES, CFD can compute the dynamic airflow and temperature variations during the day. The computations show a good agreement with the measurements, as partially evidenced by comparing the computed and measured air velocity profiles in the room as shown in Figure 11.

4. Coupled Simulation of Cooling Load for An Indoor Auto-Racing Complex

The validations verify the good performance of the coupled program developed. The coupled simulations provide more accurate and informative predictions on building thermal and airflow behaviors than the separate simulations. To demonstrate the application of this program for practical building design, this study applies the coupled program to calculate the cooling load for an indoor auto-racing facility. The facility is primarily a single space building with a floor area of over $2x10^5$ m^2 and a ceiling height of 46 m, as illustrated in Figure 12. The space can accommodate up to 60,000 spectators in the grandstands and 60,000 spectators in the infield, as well as a maximum of 45 racing cars running simultaneously on the track at an average speed of 217 km/h (135 mph).

Modeling of this facility is quite challenging and a coupled simulation of CFD and ES is indispensable because:

(1) The convective heat from the enclosures, although smaller than the enormous amount of heat from spectators, lights and cars, is still considerable because of the unusual surface convective heat transfer coefficients. The coefficients may be significantly large due to the strong forced convection caused by the racing cars.
(2) The indoor environment is not well mixed since conditioned air is only supplied to the occupant zones in such a large space to reduce the total energy consumption.
(3) Even 1% prediction error of the energy cost is considerable (around 300kW) due to the large capacity of the facility.

This study simulated the building with a three-hour racing event between 10:00-13:00 of the summer design day. The maximum spectators and racing cars were included to represent the worst scenario. Since one CFD calculation even with steady-state conditions may take about 10 hours to obtain a reasonable result for this case with a coarse grid resolution of 100×100×55, it is impractical to perform any dynamic coupling process. The study adopted the two-step static coupling process. In this ES-CFD-ES two-step static coupling, ES first calculated the surface temperatures and cooling loads using the default convective heat transfer coefficient correlations. With importing the surface temperatures and cooling loads of the peak load period as boundary conditions, CFD calculated the heat and airflow distributions in the space. The indoor air temperature gradients and convective heat transfer coefficients obtained from the CFD results were then fed back to ES to obtain more accurate cooling loads. Although the CFD results are obtained at a particular load condition (i.e., peak load), it is still reasonable to use them for the three racing hours. This is because the environmental and occupying conditions have little or no change during the racing hours, and the indoor airflow patterns dominated by the car movements can quickly reach a quasi-steady state.

The study shows that the indoor air temperature will take about an hour to reach the setup temperature of 30°C due to the thermal capacity of building envelopes and spectator seats that will store the heat gained from various heat sources (occupants, cars, lights, equipment, solar, etc.) and release them at a later time. The coupled simulation produces a longer time lag, about 20-30 minutes than the non-coupled simulation. It implies that thermal storage effect obtained in the coupled simulation is stronger than that in the non-coupled simulation. This results in a considerable decrease of the supply cooling energy, as seen in Figure 13. The total cooling energy consumed during the racing event computed by the coupled simulation is 117 GJ (32,500 kW-hour), which is about 39% less than that computed by the non-coupled simulation or 162 GJ (45,000 kW-hour).

This significant distinction is primarily due to the different surface convective heats obtained, which determine the effectiveness of the heat transfer between the indoor air and thermal masses. The coupled simulation produces much higher convective heats from all the rigid surfaces than the non-coupled ones because of the larger convection coefficients and the indoor air temperature gradients from CFD results, as presented in Table 3. The coefficients from ES are undoubtedly too small for such a strong forced convection case, while those from CFD seem more reasonable. The convective heat transfer coefficient on the west wall is about the same as that from ES due to the low air velocity behind the grandstands. The figure also reveals that the ground slab works as the most important heat reservoir during the racing event. The heat will be released to the indoor space and/or the deep ground at a later time after the racing event.

This application case further demonstrates the importance of using coupled simulation for buildings with large indoor air movement and air temperature stratification. The simulation with the static coupling strategy provides a basic and reasonable estimate of building energy consumption. More accurate results for building envelopes, indoor environmental quality and energy consumption can be obtained through the dynamic coupling. However, it is may need

excessive computing time for cases with large computational domains with a reasonable computing grid distribution.

5. Conclusions

This investigation has developed a coupled program of building energy simulation and CFD computation, incorporating all the coupling strategies and data exchange methods proposed previously by the authors. This study has validated the coupled program against the experimental data obtained from the literature for four experimental facilities. The validations verify that the program developed can provide reasonable and reliable predictions on building performance. In general, the coupled simulation produces more accurate and detailed results than the separate simulations because:

(1) CFD receives more precise and real-time thermal boundary conditions and can predict the dynamic indoor environment conditions that are important for the assessment of indoor air quality and thermal comfort.
(2) ES obtains more accurate convection heat from enclosures and can provide more accurate estimation of building energy consumption and dynamic thermal behaviors of building envelopes.

The study has found that indoor air temperature gradient and convective heat transfer coefficient have great impact on the whole building simulation. The empirical coefficient correlations used ordinary energy simulation programs may significantly deviate from the real values. The coupled simulation should be used for buildings with large indoor air temperature stratifications and/or perceptible indoor air movement.

The study has also revealed that a coupled simulation took much longer computing time than energy simulation alone. The dynamic bin coupling method may substantially reduce the computing cost while still providing reasonable results, if the changes of environmental and operational conditions between days are small.

References

Table 1 Some typical functions of ES and CFD programs for building performance studies

	ES	CFD
Weather and solar impact	Yes	No
Enclosure thermal behaviors	Yes	No
HVAC system capacity	Yes	No
Energy consumption	Yes	No
Thermal comfort (Air temperature, air velocity, air humidity, and airflow turbulence)	No	Yes
Indoor air quality (Contaminant concentrations)	No	Yes
Air distribution	No	Yes

Table 2 Summary of the coupling methods between ES and CFD and their performance

	ES to CFD	CFD to ES	Convergence	Stability	Speed	Remarks
Method-1	$T_{surface}$	h & T_{air}	★★★	★★★	★★★	Unconditional convergence Implicit iteration of T_s in ES
Method-2	$T_{surface}$	$h_{nominal}$	★★	★★	★★★	Negative h and singularity
Method-3	$T_{surface}$	$Q_{convection}$	★★	★★	★	Conditional convergence Explicit iteration of T_s in ES
Method-4	$Q_{convection}$	h & T_{air}	★	★	★	Convergence problem
Method-5	$Q_{convection}$	$h_{nominal}$	★	★	★	Negative h and singularity Convergence problem

Table 3 The computed indoor air temperature gradients, ΔT, and convective heat transfer coefficients, h, from CFD and ES for the indoor auto-racing facility

Wall	$\Delta T=T_{air}-T_{room}$ (°C)	h from CFD (W/m^2C)	h from ES (W/m^2C)	Estimated h^* (W/m^2C)
South	-0.72	84.6	2.55	68
East	0.36	86.7	2.51	76
North	0.62	47.1	2.33	68
West	-2.63	4.1	2.32	
Ground	-0.95	240.5	1.42	76
Roof	0.18	12.5	1.45	

Note: T_{air} is the air temperature close to the surfaces; T_{room} is the air temperature in the core zone of the space; h is defined based on the surface temperature and T_{room}; h^* is estimated according to the correlation for a very strong airflow over a large plate (Lienhard 1999)

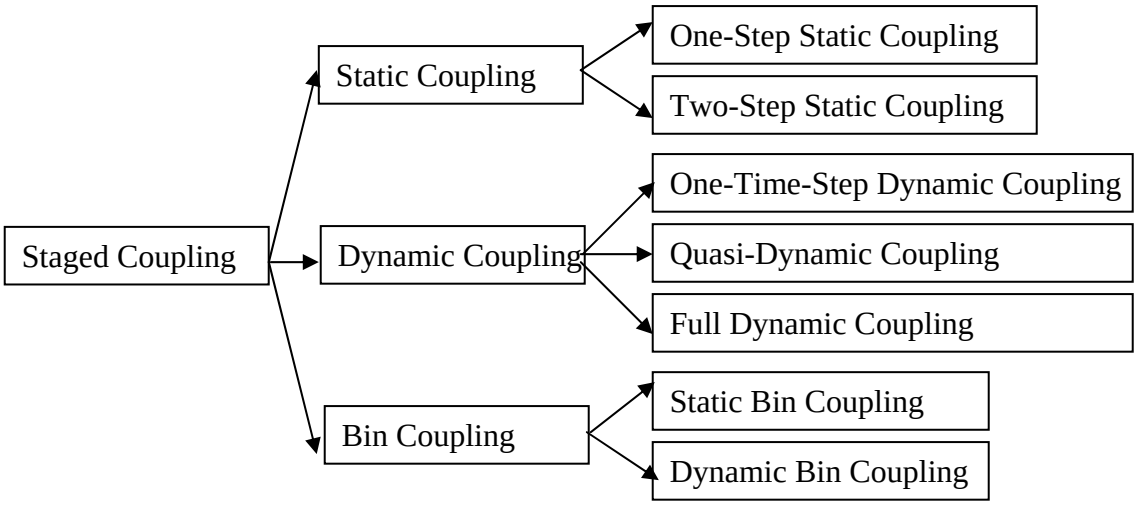

Figure 1 Tree of the staged coupling methods

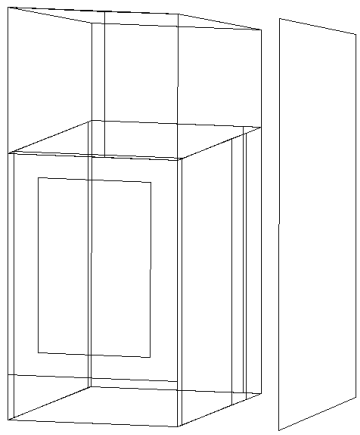

Figure 2 Computer model of IEA empirical validation test room

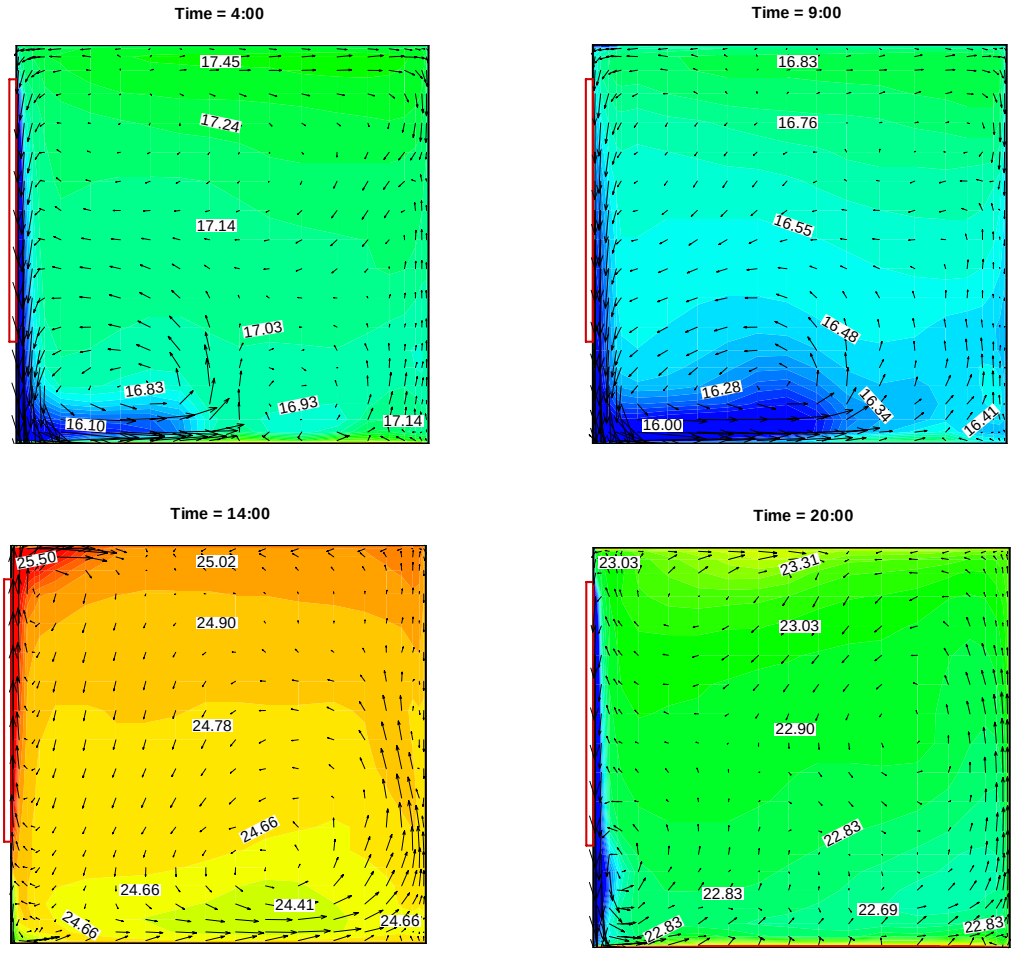

Figure 3 Airflow and temperature patterns at four different moments in the middle plane of the IEA test room without radiator

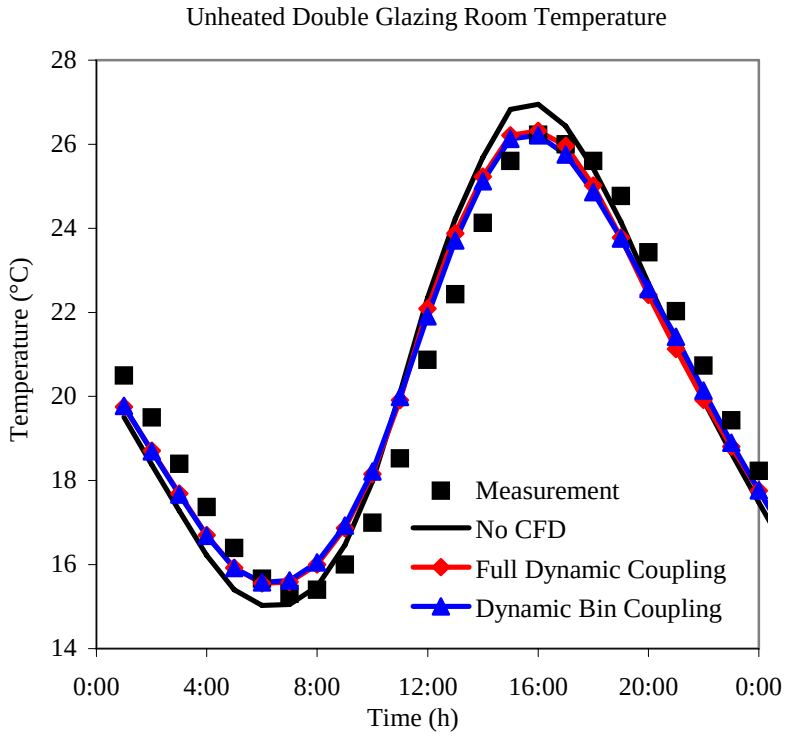

(a) from this study using E+MIT-CFD

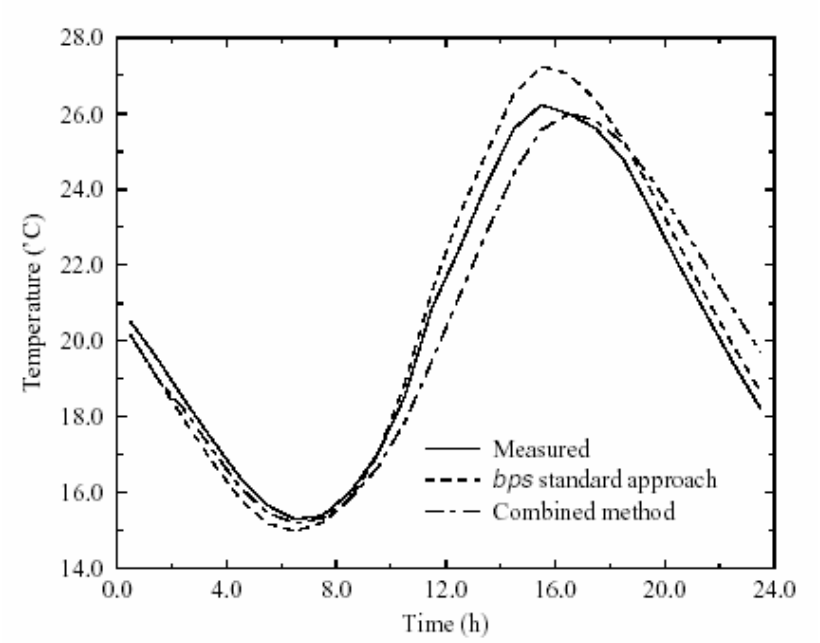

(b) from Negrao (1995) using ESP-r with CFD (bps did not use CFD option)

Figure 4 Computed and measured mean air temperature for the IEA test room without radiator

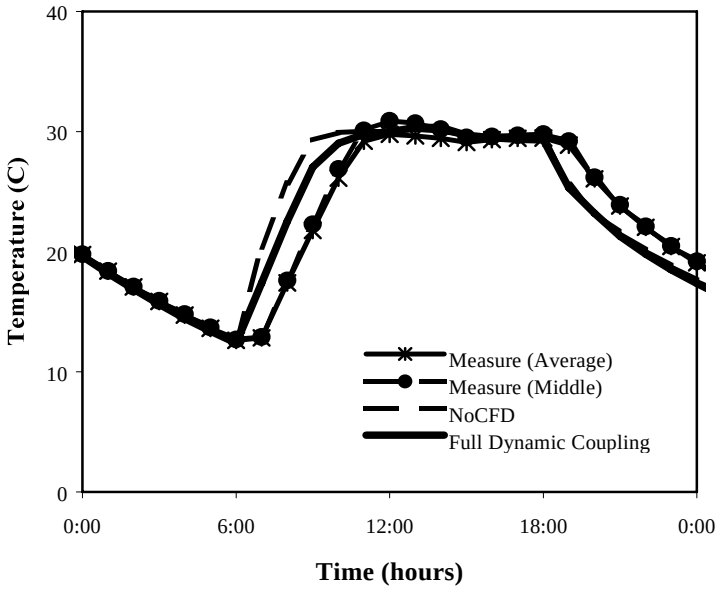

(a) from this study using E+MIT-CFD

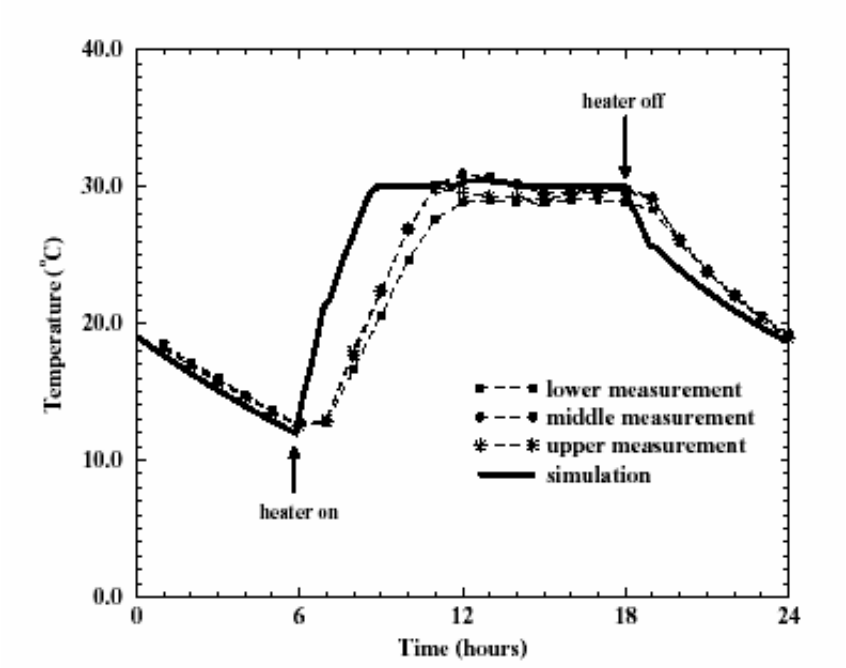

(b) from Beasoleil-Morrison (2000) using ESP-r with CFD

Figure 5 Computed and measured mean air temperature for the IEA test room with radiator

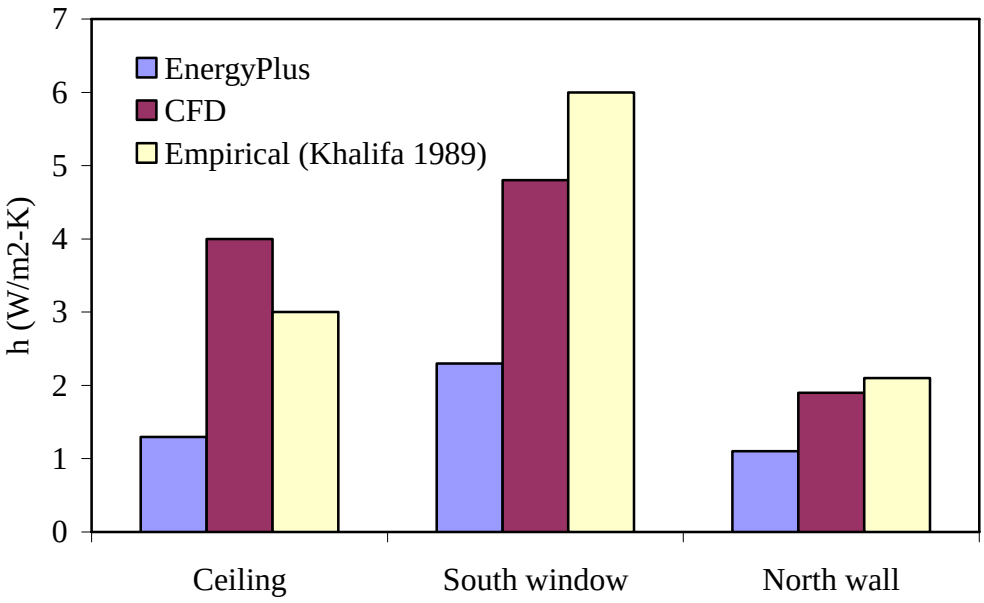

Figure 6 Daily-averaged convective heat transfer coefficients determined for the IEA test room with a radiator underneath the south window

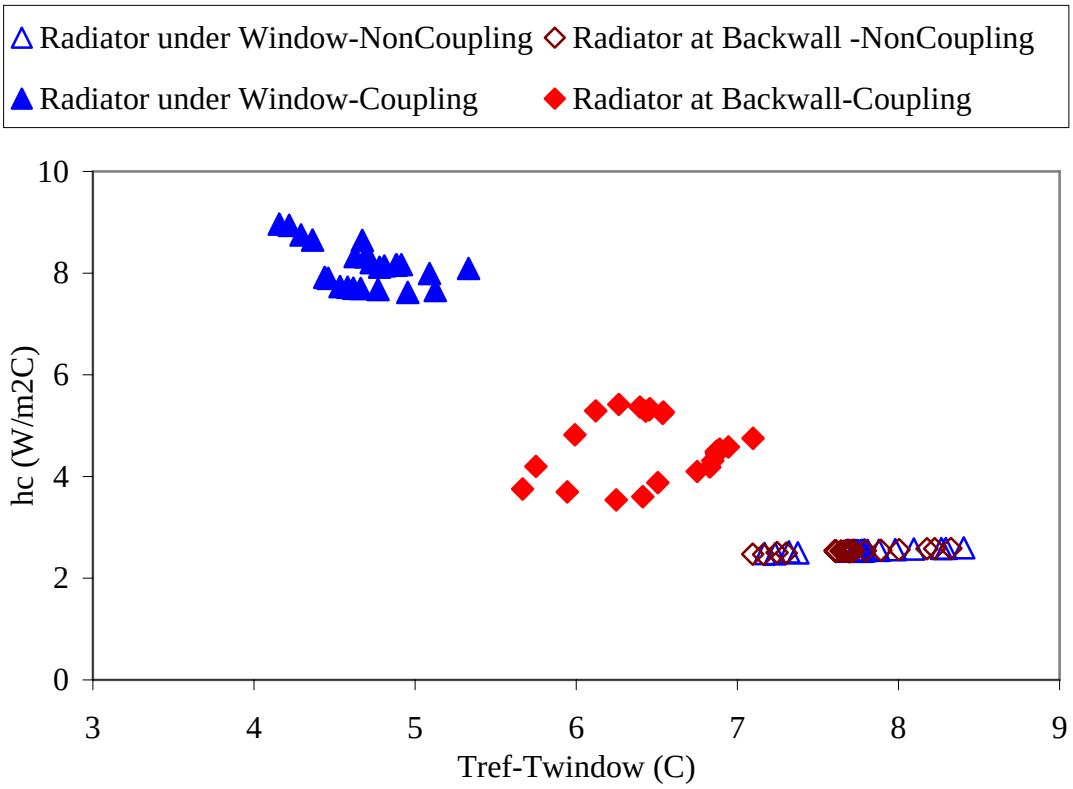

Figure 7 Simulated convective heat transfer coefficients, h_c, at the south window of a test room used by Wallenten (1998)

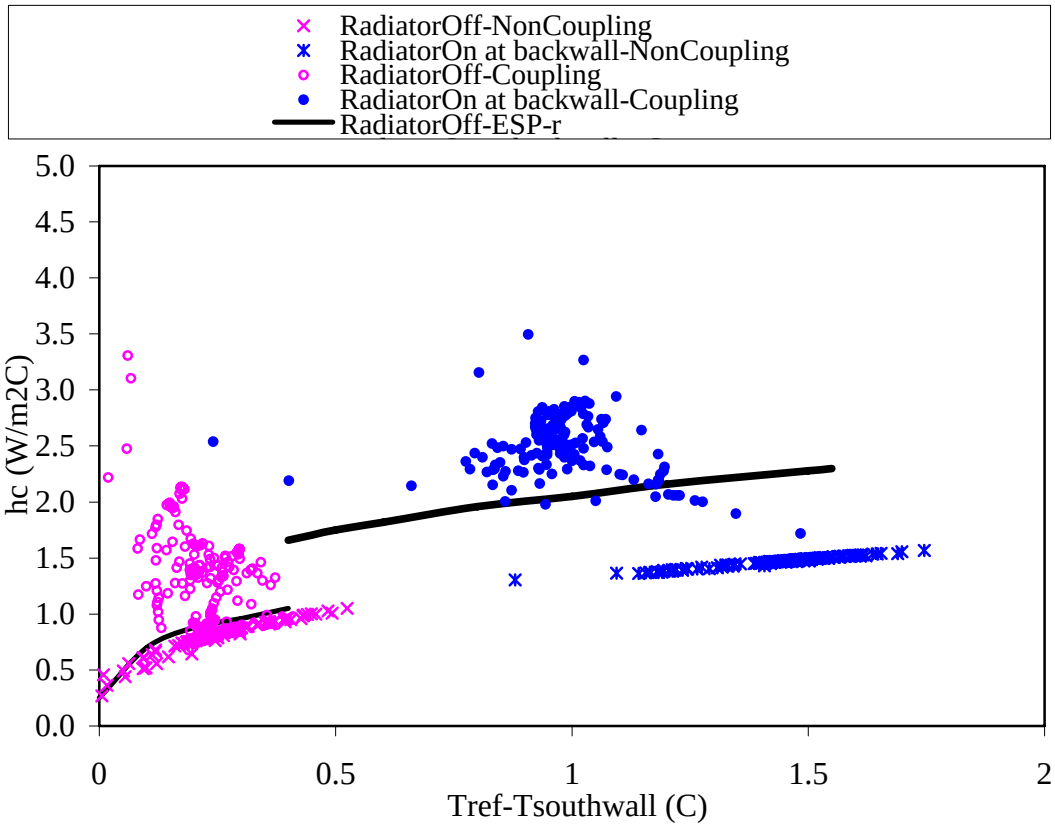

Figure 8 Comparison of the computed convective heat transfer coefficient, h_c, at the south wall between the current study and that from Beausoleil-Morrison (2000) when the radiator is at the back wall of Wallenten's test room

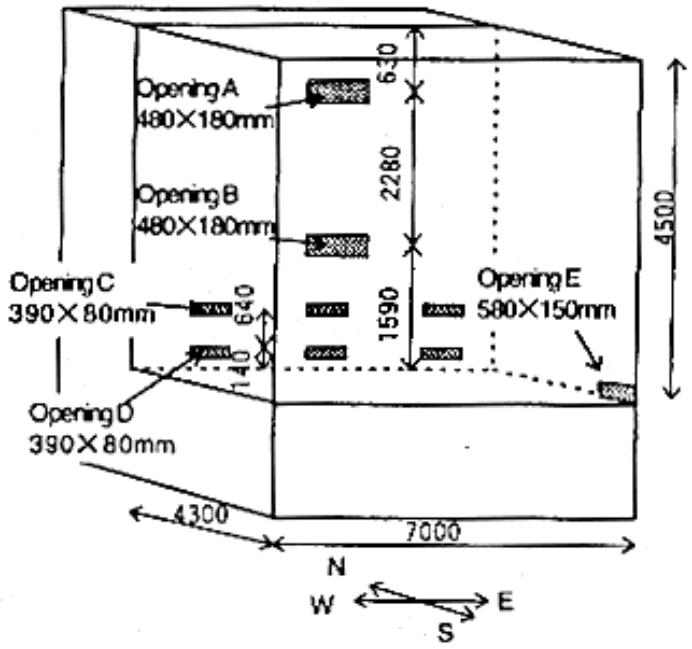

Figure 9 The size and openings of the experimental glazed atrium (Hiramatsu et al 1996)

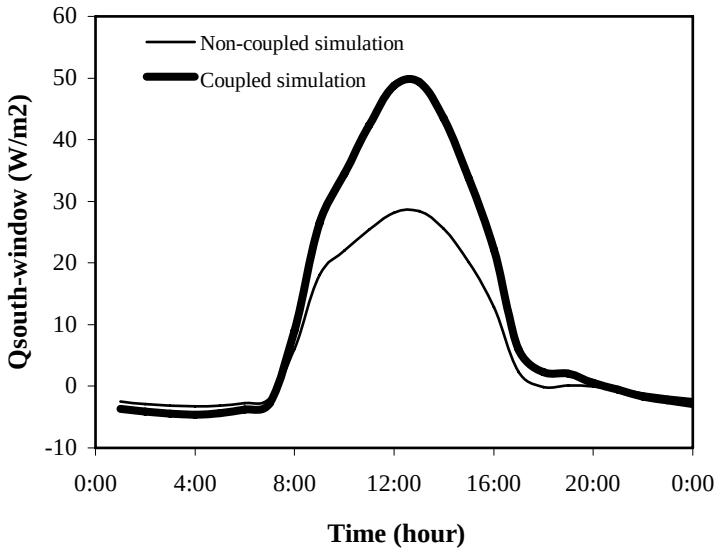

(a) Calculated convective heat from the south window of the atrium

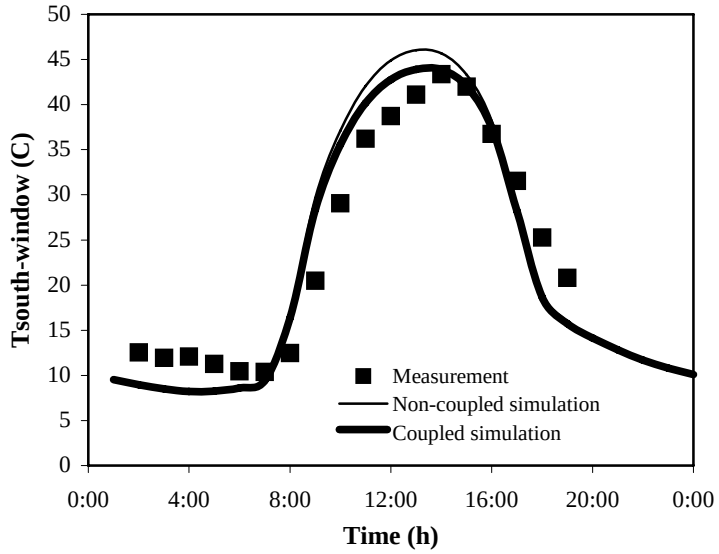

(b) Calculated and measured south window interior surface temperature

Figure 10 Convective heat and temperature on the south window of the atrium.

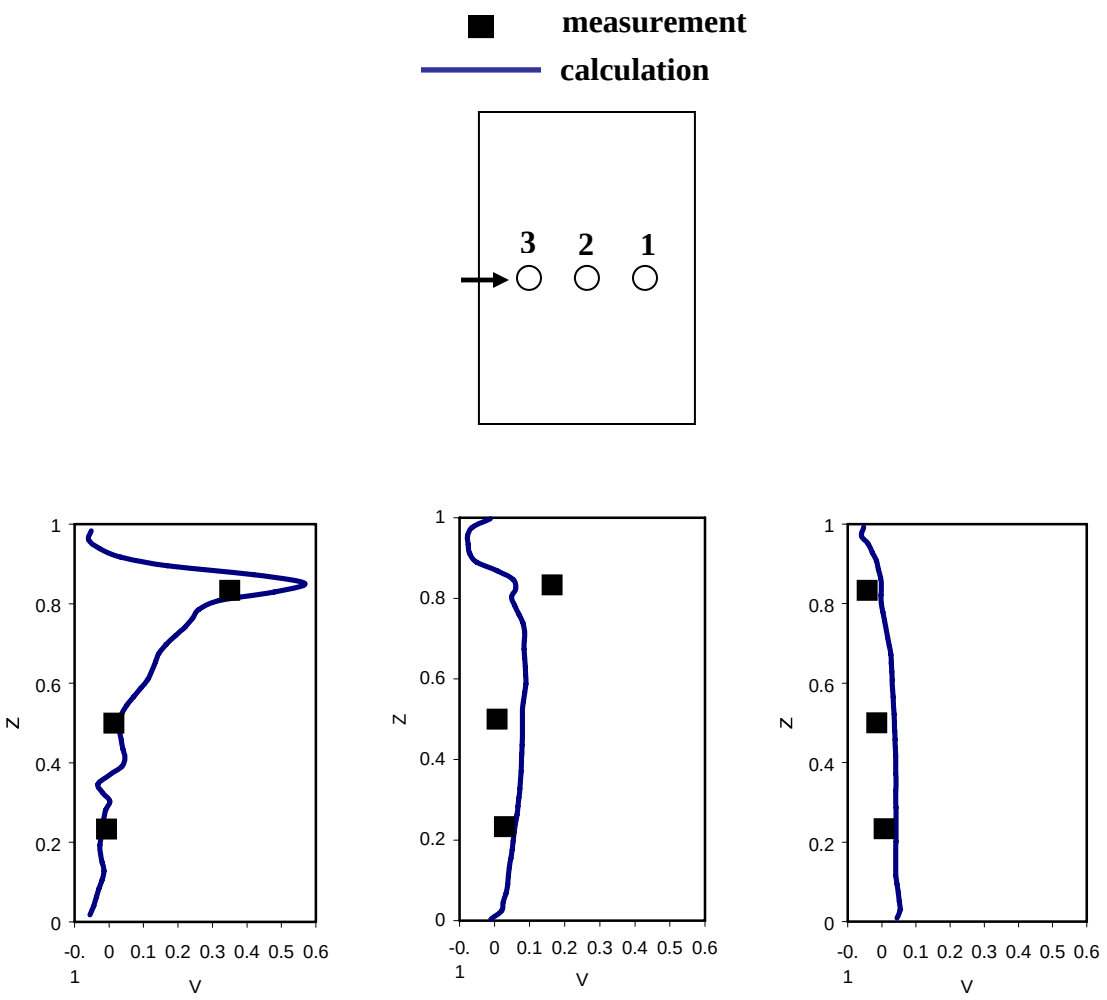

(a) Velocity profiles at 8:00 AM

(b) Velocity profiles at 10:00 AM

Figure 11 Computed and measured air velocity profiles in three different locations in the atrium (Z=height/H, $V=V_{air}/V_{in}$)

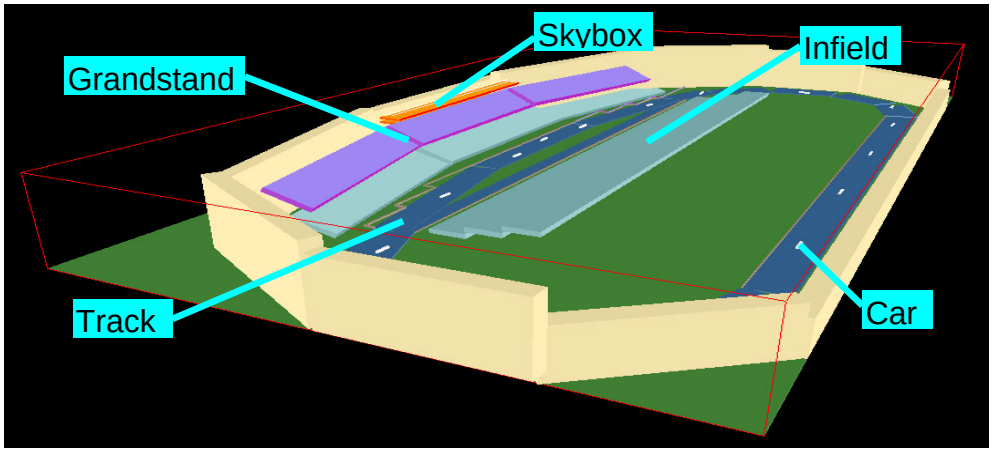

Figure 12 Computer model of the indoor auto-racing complex

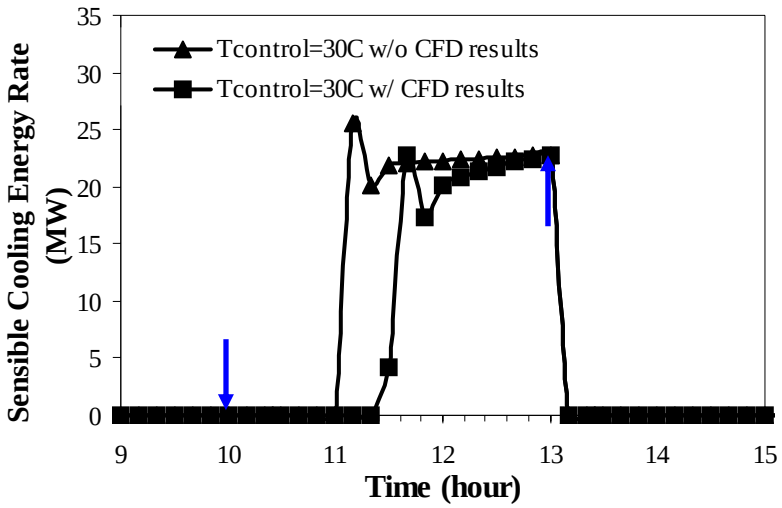

Figure 13 Sensible cooling energy rate during the racing event computed with and without CFD results